Journal of Materials Chemistry A

Accepted Manuscript

This article can be cited before page numbers have been issued, to do this please use: S. H. Kim, J. S. Yeon, R. Kim, K. M. Choi and H. S. Park, *J. Mater. Chem. A*, 2018, DOI: 10.1039/C8TA08843H.

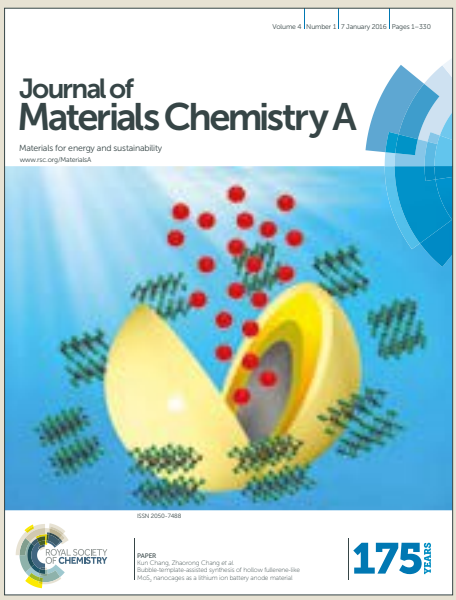

ROYAL SOCIETY OF CHEMISTRY

rsc.li/materials-a

View Article Online
DOI: 10.1039/C8TA08843H

Journal Name

ARTICLE

Functional Separator Coated by Sulfonated Metal Organic Framework/Nafion Hybrids for Li-S Batteries

Seon Hwa Kim[a,‡], Jeong Seok Yeon[a,‡], Raekyung Kim[b], Kyung Min Choi[b,*], and Ho Seok Park[a,c,*]

Received 00th January 20xx,
Accepted 00th January 20xx

DOI: 10.1039/x0xx00000x

www.rsc.org/

Functional separator is designed to improve the utilization of sulfur and to inhibit polysulfide shuttling for high performacne lithium-sulfur (Li-S) batteries. Here, we demonstrate a functional separator which is coated by sulfonated UiO-66 metal organic framework (MOF)/Nafion on a polyethylene separator. This modified separator acts as suppressing the polysulfide diffusion due to a molecular sieving and electrostatic repulsion effect and facilitating the redox kinetics of sulfur conversion because of a fast charge tranport by sulfonic groups tethered to MOF and Nafion. Thus, the Li-S cells based on the MOF/Nafion hybrid-coated separator achieve the discharge capacity of 1127.4 mAh g^{-1} at 0.1C, the capacity retention of 66.8 % at 3C relative to 0.1C, and the cyclic stability of 75.5% over 200 charging/discharging cycles. These values are much greater than those of pristine and Nafion-coated separators, which confirms the superiority of MOF/Nafion hybrid coating layers for the design of functional separator.

Introduction

The development of advanced energy storage systems with a high energy density and a low cost is motivated by the rapidly increasing demands on the renewable energy storage and electric vehicles. To achieve this goal, the lithium-sulfur (Li-S) batteries are considered as a promising option. In particular, the cost-effective sulfur cathodes accommodate the large amounts of lithium (Li) ions *via* a conversion reactions, thereby achieving a high theoretical capacity of 1672 mAh g^{-1}.[1] However, this mechanism simultaneously causes the critical problem such as the shuttle effect of polysulfides. Long-chain polysulfides (S_n^{2-}, $4<n\leq8$) can be easily dissolved in the commonly used organic electrolytes and crossover from cathode to anode under a concentration gradient.[2] Thus, this shuttling process causes unfavourable effects such as a self-discharging, low coulombic efficiency, poor cycle stability and loss of active sulfur materials.[3, 4]

To suppress this effect, many researches have focused on confining the sulfur within the cathode region.[5-10] Among various hosts such as porous carbon[5, 6], metal oxide[7, 8], and conducting polymer[9, 10], metal organic frameworks (MOFs), which are highly porous materials composed of organic-inorganic hybrid structure, can achieve outstanding polysulfides trapping capability of their metallic centers based on Lewis acid-base interaction.[11] Tarascon et al. suggested a MOF/sulfur composite cathode in 2011, demonstrating its remarkable increase in capacity retention for Li-S batteries.[12] Although accommodating sulfurs into host materials is an effective way to improve the performances of Li-S cells, the reduction of active material loadings results in lowering an energy density.[13] The modification of separator is proposed to resolve both issues of polysulfide shuttling and reduced energy density, taking advantage of cost-effective process. For instance, Manthiram et al. demonstrated a conductive carbon-coated separator, serving as an upper current collector to reactivate the dead sulfur as well as a physical barrier to inhibit polysulfide shuttling.[13] In addition to a physical barrier effect, introducing negatively charged functional groups to the coated layer is also an effective way to resolve the aforementioned problems. The sulfonic groups ($-SO_3H$) of multiwall carbon nanotube/sulfonated polyaniline coated on separator inhibited polysulfide shuttling *via* an electrostatic repulsion with polysulfide anions.[14] Likewise, Huang et al. reported Nafion-coated polypropylene separator for the greatly enhanced performances[15], because Nafion acts as an ion selective membrane.[16, 17] Nonetheless, most of the separator modifications showed the physical blocking or strong anchoring to prevent polysulfide shuttling, yet there are a few ones enhancing the redox kinetics and reversibility of polysulfide conversion reaction.

Herein, we report an improved kinetics and polysulfide inhibition developing MOF/Nafion hybrid-coated separator. In particular, sulfonic-acid functionalized UiO-66 (UiO-66-S), which is MOF $[Zr_6O_4(OH)_4(BDC)_6$ (BDC = 1,4- benzenedicarboxylate), termed UiO-66] with functional group of sulfonic acid ($-SO_3H$),[18, 19] is used because its pore sizes (of 11 and 8Å) are

[a] School of Chemical Engineering, College of Engineering, Sungkyunkwan University, 2066, Seobu-ro, Jangan-gu, Suwon-si, Gyeonggi-do 440-746, Republic of Korea
[b] Department of Chemical and Biological Engineering, Sookmyung Women's University, 100 Cheongpa-ro 47 gil, Yongsan-gu, Seoul 04310, Republic of Korea
[c] SKKU Advanced Institute of Nanotechnology (SAINT), College of Engineering, Sungkyunkwan University, 2066, Seobu-ro, Jangan-gu, Suwon-si, Gyeonggi-do 440-746, Republic of Korea
‡These authors are equally contributed

Electronic Supplementary Information (ESI) available: [details of any supplementary information available should be included here]. See DOI: 10.1039/x0xx00000x

View Article Online
DOI: 10.1039/C8TA08843H

much smaller than the size of polysulfides (S_n^{2-}, 4<n≤8) and the sulfonated derivatives promote electrostatic repulsion with polysulfide anions and ionic conduction for lower polarization.[20, 21] Thus, the Li-S cell using the UiO-66-S/Nafion hybrid-coated separator was able to restrict polysulfide shuttling and to promote the redox kinetic of sulphur conversion for the improved capacity, reversibility, rate capability, and long cyclic stability.

Experimental section

Preparation of UiO-66-S

UiO-66-S was synthesized following our previous report.[22] $ZrCl_4$ (34.9 mg, 0.15 mmol, Aldrich), H_2BDC (18.8 mg, 0.113 mmol, Aldrich) and Monosodium salt of 2-sulfonyl terephthalic acid (10 mg, 0.037 mmol, TCI), and acetic acid (0.7 mL) were mixed in DMF (Aldrich). The vial was sealed with a Teflon cap and heated for 24 hours at 120 °C. The product was suction filtered and washed with DMF and methanol, then followed by vacuum drying.

Preparation of UiO-66-S/Nafion hybrid-coated separator

The commercial polyethylene membrane (SK innovation) was employed as the pristine separator. The fabrication process of UiO-66-S/Nafion hybrid-coated separator is shown in Fig. S1. UiO-66-S was dispersed in isopropanol by sonication for 3 hours, then stirred with Nafion solution (Sigma-aldrich) for 1 hour. Vacuum filtration was carried out to uniformly coat the UiO-66-S/Nafion hybrid layer onto the pristine separator. The loadings of UiO-66-S and Nafion were 0.1 and 1.0 mg cm^{-2} respectively. Remaining solvents were dried at room temperature in the air. The pristine and Nafion-coated separators were also prepared to compare the performances of the UiO-66-S/Nafion hybrid modified separator.

Preparation of reduced graphen oxide/sulfur composite

Graphene oxide (GO) dispersion was prepared by using a Hummer's method.[23] The obtained GO was homogeneously dispersed in water at a concentration of 5 mg ml^{-1}, then the freeze-dried. The as-obtained GO powder was thermally treated at 900℃ for 2 hours under argon atmosphere. The reduced GO (rGO) powder to elemental sulfur (Sigma-aldrich) at a weight ratio of 1 to 2.5 were evenly mixed in mortar for 1 hour. The mixture was then transferred into a sealed container filled with argon and heated at 155℃ for 9 hours and 160℃ for 2 hours. TGA analysis confirmed that a rGO/sulfur composite contained 70.5 wt% of sulfur (Fig. S2).

Characterization

Scanning electron microscopy (SEM) images of the separators were obtained by a field emission SEM (GENESIS 2000, LEO SUPRA 55). Attenuated total reflection (ATR) mode was employed to measure the Fourier transform infrared (FT-IR) spectra. X-ray diffraction (XRD) patterns of the separators were taken by a D8 advance diffractometer (Bruker, Germany) in a 2θ range from 5 to 30°.

Electrochemical measurement

To measure the Li-S cell performance of three separators, CR2032 half-cell test was conducted. All cells were assembled in an argon-filled glove box at the concentrations of O_2 and H_2O below 0.1 ppm. The cathodes were prepared by mixing the active material of the rGO/sulfur (80wt%), carbon black (10wt%), and polyvinylidene fluoride (PVDF, 10wt%), followed by adding an appropriate amount of N-methyl-2-pyrrolidinone in order to form a homogeneously slurry. After that, the slurry was coated on Al foils using a bar-coater and dried over night at 80℃. Then electrodes were cut into circular disks with 1.7 mg cm^2 of sulfur loading. The metallic lithium (Lithium foil, Alfa Aesar) with 19 mm diameter and 0.75mm thickness was used as anode. The electrolyte solution consisted of 1M lithium bis(trifluoromethylsufonyl)imid (LiTFSI, Sigma-aldrich) dissolved in 1,3-dioxolane (DOL, Sigma-aldrich)/1,2-dimethoxyethane (DME, Sigma-aldrich) (1:1 v/v). The UiO-66-S/Nafion hybrid coated separator was placed on the electrode and then, 17 μl of electrolyte solution was added to the cell (E/S ratio < 10:1). Cycling voltammetry tests were conducted using a Bio-Logic instrument (VMP3 potentiostat/galvanostat with EIS) from 1.5 to 3.0 V in the following cycles with a scan rate of 0.1mV s^{-1}. Electrochemical impedance spectroscopy (EIS) measurements, which are same model as above, were performed in the frequency range of 10^3kHz to 10^{-2}Hz at open-circuit voltage. Galvanostatic charge-discharge (GCD) data were collected at various current densities within a voltage range of 1.5-3.0 V using Maccor instrument (Series400 automated test system). The capacities and current densities were calculated based on the mass of sulfur content in the cathode. (1C = 1672 mAh g^{-1}) For comparison, Li-S cells with pristine and only Nafion coated separators were also assembled in the same way and tested under the same conditions as mentioned above.

Permeation test

Visible experiment of long-chain polysulfide diffusion was conducted to test the permeability of each separator. Long-chain polysulfide solution (0.025 M Li_2S_6) was prepared mixing sulfur powder with Li_2S in a DOL/DME (1:1 v/v) for 72h.[24] Vial containing Li_2S_6 solution was sealed with each separator and immersed reversely in the empty DOL/DME (1:1 v/v) solution. The test was carried out in a glove box filled with argon gas and there is no external pressure during the experiment.

Result and discussion

Since polysulfides pass through the separator channels to react with the Li metal anode,[16] the porous and surface structures of separator need to be characterized. The porous structure of pristine separator was confirmed as shown in Fig. 1a. The porous surfaces of pristine separator are uniformly covered by coating either Nafion or UiO-66-S/Nafion hybrid layer (Figs. 1c and 1e). On the other hand, UiO-66-S particles

View Article Online
DOI: 10.1039/C8TA08843H

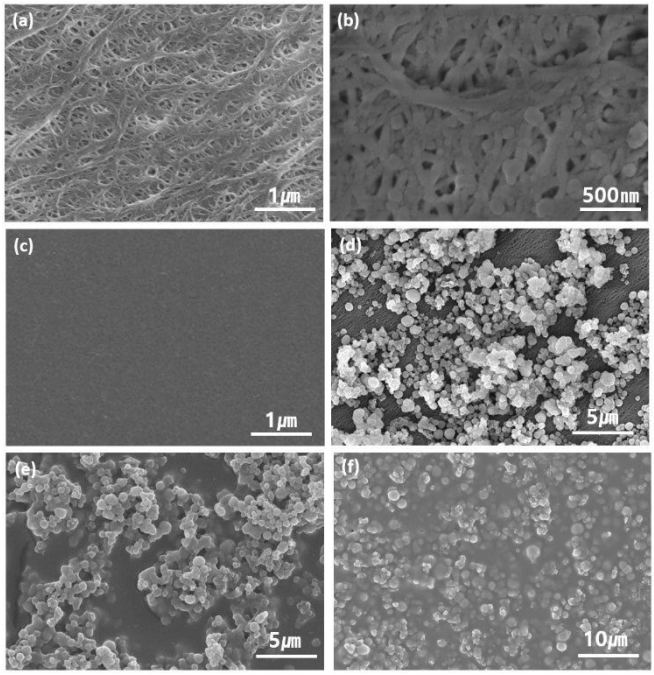

Fig. 1 SEM images of (a, b) pristine separator before and after cycling process, (c) Nafion-coated separator, (d) UiO-66-S-coated separator, and (e, f) UiO-66-S/Nafion hybrid-coated separator before and after cycling process.

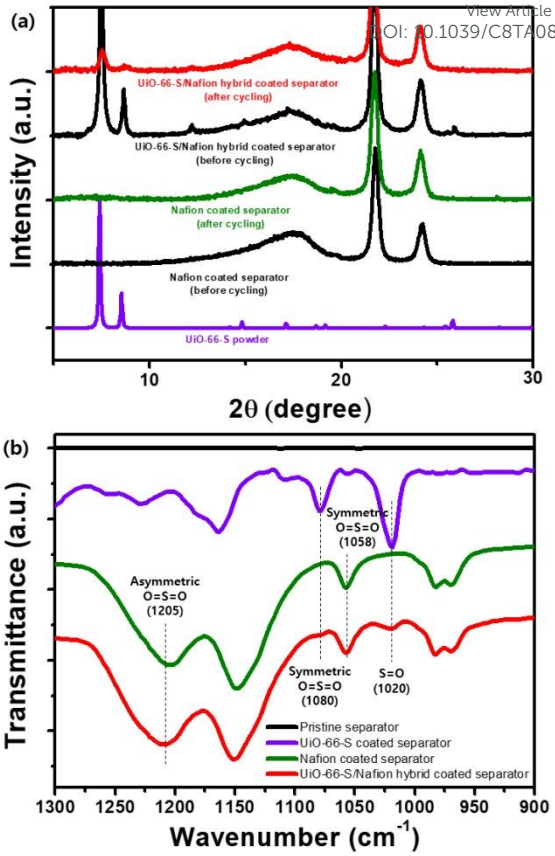

Fig. 2 (a) XRD patterns of Nafion- and UiO-66-S/Nafion hybrid-coated separators before and after cycling process. (b) FTIR spectra of pristine, Nafion-coated, UiO-66-S-coated, and UiO-66-S/Nafion hybrid-coated separators.

could not completely coat the porous channels of pristine separator (Fig. 1d). The Nafion coated separator showed non-porous structure, while the UiO-66-S/Nafion hybrid-coated separator still exhibited porous surface due to the existence of MOF particles. All the thicknesses of Nafion, UiO-66-S, and UiO-66-S/Nafion hybrid coating layers were almost identical within the marginal range of 4 μm to focus the effect of MOF on the shuttling inhibition.

The XRD analysis was conducted to confirm the crystalline structure of MOF. As presented in the Fig. 2a and Fig. S3, the XRD pattern of Nafion coated separator showed a broad peak at 2θ=17.3° corresponding to amorphous halo. On the other hand, the XRD pattern of UiO-66-S/Nafion hybrid-coated separator exhibited two intensive peaks at 2θ=7.3° and 2θ=8.5°, which were assigned to the octahedral and tetrahedral cages of (111) and (200) planes, respectively.[25, 26] The crystalline structure of UiO-66-S was well preserved for UiO-66-S/Nafion hybrid. The sulfonic groups of UiO-66-S/Nafion hybrid-coated separator were identified by Fourier transform infrared (FTIR) spectroscopy, as shown in Fig. 2b. The FTIR spectrum of Nafion-coated separator showed two peaks at 1205 and 1058 cm^{-1}, which were assigned to asymmetric and symmetric stretching vibrations of O=S=O, respectively.[27] Likewise, UiO-66-S coated separator also identified the sulfonic groups observing peaks at 1088 and 1020 cm^{-1} corresponding to the symmetric stretching vibrations of O=S=O and the stretching mode of S=O, respectively.[28, 29] These characteristic peaks of sulfonic groups arising from Nafion and UiO-66-S were also observed in FTIR spectrum of UiO-66-S/Nafion hybrid-coated separator. However, the peak intensities of the UiO-66 were lower than those of the Nafion, because of the lower loading amount of the former. These sulfonic groups of UiO-66-S/Nafion hybrid-coated separator are capable of reactivating the dead sulfur as well as of repulsing polysulfide anions by the role as an ionic barrier.

In order to evaluate the effect of the UiO-66-S/Nafion coating on the electrochemical behaviours of Li-S cells, 2032 coin cells were assembled in a half cell of Li metal anode and rGO/sulfur composite cathode. The Li-S cells using pristine, Nafion-coated, and UiO-66-S-coated separators were tested and compared. Fig. 3a displays GCD profiles of the Li-S cells with UiO-66-S/Nafion hybrid-coated separator at 0.2C and at different cycle numbers (1st, 2nd, 10th, 50th, 100th, and 200th cycles). Two voltage plateaus of discharge curves were observed at around 2.34 and 2.06 V, which are attributed to the complex reduction reactions; sulfur is converted into long-chain polysulfides and these polysulfides are further reduced into short-chain polysulfides of Li_2S_2 and Li_2S.[30] In the charging profile, single plateau region was captured and attributed to the oxidation of Li_2S/Li_2S_2 to Li_2S_4, Li_2S_8 and further oxidation to S_8.[31]

View Article Online
DOI: 10.1039/C8TA08845H

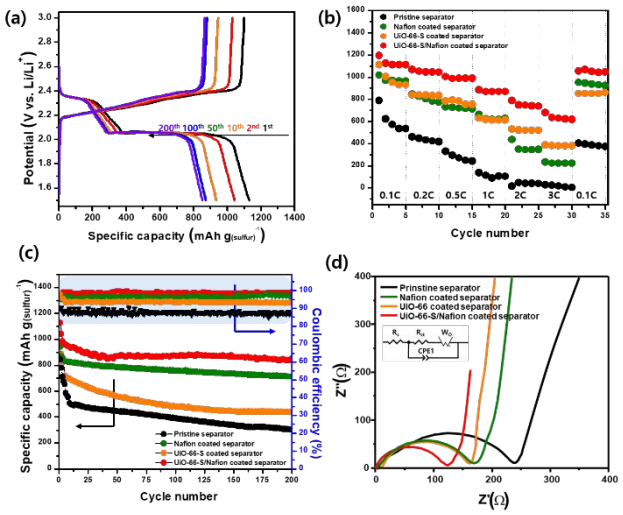

Fig. 3 (a) GCD profiles of Li-S cells with UiO-66-S/Nafion hybrid-coated separator at 0.2C. (b) Rate capabilities at various C rates, (c) Cycling performances and Coulombic efficiencies at 0.1C, and (d) Nyquist plots of Li-S cells with pristine-, Nafion-coated, UiO-66-S-coated, and UiO-66-S/Nafion hybrid-coated separators. Inset of Fig. 3d indiates equivalent circuit model.

These charging/discharging plateaus with minor voltage hysteresis were kept almost the same during a cycling process despite the decrease in the capacity. By contrast, the Li-S cell with the pristine separator showed a dramatic capacity fading and serious polarization during a cycling process, while that with Nafion-coated and UiO-66-S-coated separators also revealed a relatively severe capacity fading and polarization than those with the UiO-66-S/Nafion hybrid-coated separator (Fig. S4). The specific discharge capacity of the Li-S cell with the UiO-66-S/Nafion hybrid-coated separator was 1185 mAh g^{-1}, which was greater than 787, 1017, and 1109mAh g^{-1} with the pristine, Nafion-coated, and UiO-66-S-coated separators as shown in Fig. 3b. When the rates increased from 0.1 to 3C, the discharge capacity was reduced into 785 mAh g^{-1} with the rate capability of 66.2 %. These 3C capacity and rate capability were much better than 28.8 mAh g^{-1} and 3.7 % with the pristine separator, 234.8 mAh g^{-1} and 23.0 % with the Nafion-coated separator and 385.2 mAh g^{-1} and 34.7 % with the UiO-66-S-coated separator, respectively. Despite different measurement conditions and samples, Li-S cell with UiO-66-S/Nafion hybrid coated separator exhibited the highest specific capacity and rate capability among previously reported works using MOF-modified separators (Table. S1).[43-48] Even when getting back to 0.1 C, a high reversible capacity of 1056 mAh g^{-1} was achieved. Furthermore, plateaus regions with insignificant polarization were well preserved up to 3C charging/discharging (Fig. S5).

As show in Fig. 3c, the cycling performances of the four Li-S cells were measured over 200 charging/discharging cycles at 0.2 C. The initial discharge capacity of 845.7 mAh g^{-1} for the Li-S cell with pristine separator was rapidly dropped to 500.2 mAh g^{-1} at the 10th cycle. Then, the capacity was steadily decayed down to 301.4 mAh g^{-1}, 35.6 % of the initial value, at the 200th cycle. The cycling performance of the Li-S cells with UiO-66-S-coated separator was slightly higher than that with the pristine separator but lower than those with Nafion-coated and UiO-66-S/Nafion hybrid-coated separators due to incomplete coating of UiO-66-S MOF, showing 46.2 % of capacity retention from 947.5 to 437.6 mAh g^{-1} over 200 cycles. For the Nafion-coated separator, the cycling performance of the Li-S cells was improved, showing 75.8% of capacity retention from 938.6 to 712.2 mAh g^{-1} over 200 cycles. This finding was due to the electrostatic repulsion by the Nafion coating layer to prohibit the polysulfide shuttling.[17] The cycling performance was further improved when the UiO-66-S/Nafion hybrid was coated. The capacity retention of 77.4% from 1127.4 to 872.3 mAh g^{-1}, corresponding to a decay rate of 0.11% per cycle, was achieved by the UiO-66-S/Nafion hybrid-coated separator. As shown in the Coulombic efficiency, the reversibility of the Li-S cell with the UiO-66-S/Nafion hybrid-coated separator (98.0 % of the Coulombic efficiency) was better than those with the pristine, UiO-66-S-coated and Nafion-coated separators (90.3, 95.5 and 97.8 % of the Coulombic efficiencies). In addition, the cyclic stability of the Li-S cells with each separator were further tested over 1,000 cycles at 1C after activation process at 0.1 C for the initial three cycles. The Li-S cell with UiO-66-S/Nafion hybrid-coated separator showed a lower capacity fading rate of 0.032 % per one cycle over 1,000 cycles than those with pristine (0.07 % per one cycle over 300 cycles), UiO-66-S-coated (0.064 % per one cycle over 1,000 cycles), and Nafion-coated (0.044 % per one cycle over 1,000 cycles) separators, delievering a capacity of 654.5 mAh g^{-1} even at 1,000th cycle (Fig. S6).

The greatly improved performances such as high reversible capacity, rate capability, high energy efficiency (high Coulombic efficiency and low voltage hysteresis), and long cyclic stability were attributed to the efficient inhibition of polysulfide shuttling and facilitated redox kinetics by synergies effect with the UiO-66-S/Nafion hybrid coating. To confirm the kinetic enhancement by the UiO-66-S/Nafion hybrid coating, the Nyquist plots of three cells are obtained using impedance spectroscopy as shown in Fig. 3d. The x-intercept, semi-circle, and inclined straight line, corresponding to equivalent series resistance (R_s), charge transfer resistance (R_{ct}) and Warburg impedance (W_0), respectively,[32] are observed in the high, middle and low frequencies, respectively, and derived from equivalent circuit model. Both the Nafion, UiO-66-S and UiO-66-S/Nafion hybrid-coated separators showed steeper Warburg slopes than that of the pristine separator, indicating the rapid ion diffusion into the active sites of sulfur cathode. This finding confirmed the enhanced ionic transport by the Nafion layer despite the increased thickness. In particular, The Li-S cell with the UiO-66-S/Nafion hybrid-coated separator showed 0.6 and 123.0 Ω of R_s and R_{ct}, respectively, which were lower than those with pristine (4.8 and 273.8 Ω of R_s and R_{ct}), UiO-66-S-coated (6.5 and 171.2 Ω of R_s and R_{ct}), and Nafion-coated (1.4 and 161.3 Ω of R_s and R_{ct}) separators. This result indicates that considering the nearly identical thickness of Nafion, UiO-66-S and UiO-66-S/Naion hybrid coating layers, MOF hybridization contributed to

View Article Online
DOI: 10.1039/C8TA08455H

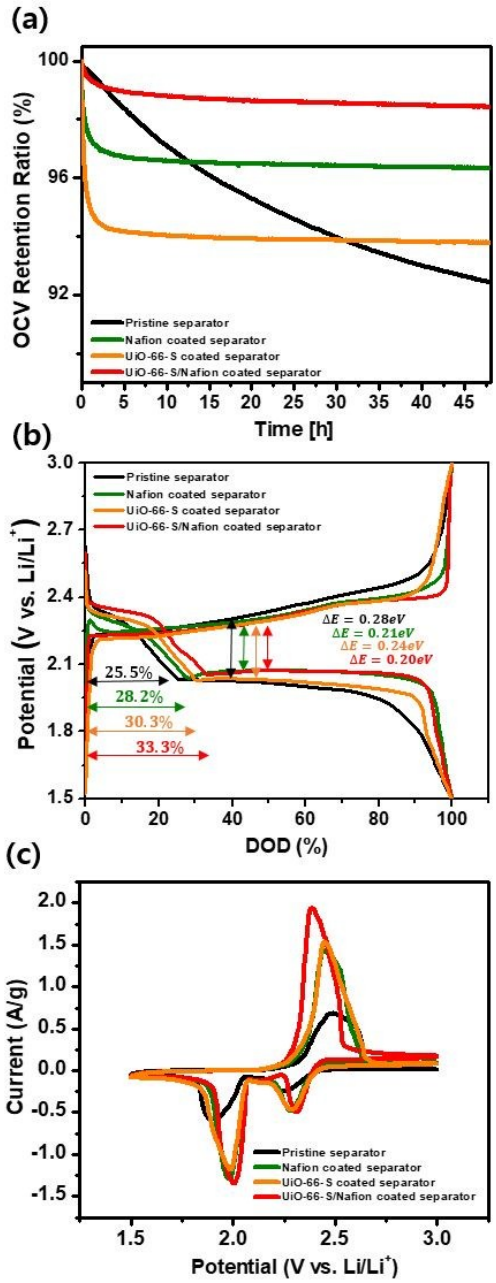

Fig. 4 (a) OCV retention ratio profiles showing self-discharge behaviour during 48h of relaxation, (b) GCD profiles at 0.1C with respect to DOD degree, and (c) 2nd cycle CV profiles at a scan rate of 0.1mV s^{-1} of Li-S cells with pristine, Nafion-coated, UiO-66-S-coated, and UiO-66-S/Nafion hybrid-coated separators.

the improved charge transfer kinetics of slow polysulfide conversion process.

The effect of UiO-66-S/Nafion hybrid coating layers on the self-discharging inhibition was studied measuring the normalized open-circuit voltage (OCV) profiles of Li-S cells during 48 hours of a resting period (Fig. 4a). The OCV of Li-S cells using pristine separator was continuously declined during the measurement. By contrast, the Li-S cells with UiO-66-S-, Nafion- and UiO-66-S/Nafion hybrid-coated separators showed 93.7, 96.3 and 98.4% of initial OCV after 48 hours, respectively. The preservation of OCV implies that both Nafion and UiO-66-S hybrid coating layers effectively inhibited polysulfides dissolution and shuttling.[33]

The polarization of conversion-based reaction was analyzed measuring GCD curves at the 1st cycle with respect to depth of discharge (DOD),[34] as shown in Fig. 4b. The voltage hysteresis of three samples is related to the polarization arising from the kinetic limitation and polysulfide shuttle effect.[35] The Li-S cell with the UiO-66-S/Nafion hybrid-coated separator showed the lower voltage hysteresis of 0.20 eV than 0.28, 0.21, and 0.24 eV with the pristine, UiO-66-S-coated, and Nafion-coated separators, respectively. The length of upper plateaus was estimated during a discharging process, where long-chain polysulfides can be produced and dissolved in the organic-electrolyte. In the case of Li-S cell with UiO-66-S/Nafion hybrid-coated separator, a long upper plateau region reached 33.3% of DOD level. This length of upper plateau was longer than those with pristine (25.5% of DOD level), UiO-66-S-coated (30.3% of DOD levels), and Nafion-coated (28.2% of DOD levels) separators. At around 100% of DOD, the Li-S cells using UiO-66-S/Nafion hybrid-coated separators showed the steepest slopes at both charge and discharge curves, where long-chain polysulfides are converted into discharged products of Li_2S_2 and/or Li_2S or vice versa.[36] Voltage drop at the lower plateau indicates that these conversions are kinetically sluggish and require more activation energy.[37] These apparent differences in voltage hysteresis, plateau length, and GCD slope were attributed to different kinetic features by means of separator modifications.

Cyclic voltammetry (CV) curves of three samples are measured to further investigate the electrochemical features of the Li-S cells with different separators, in the voltage window of 1.5 - 3.0 V at a scan rate of 0.1 mV s^{-1} for the initial ten cycles (Fig. S7). The typical two pairs of redox peaks are associated with the conversion reaction of elemental sulfur as shown in CV curves. These curve features were consistent with the results of GCD profiles in Fig. 4b. After the 1st cycle of activating process, the current and position of redox peaks almost remained intact except for the pristine separator, indicating that the electrochemical process was stabilized by Nafion and UiO-66-S hybrid coating. In the 2nd cycle (Fig. 4c), the CV curves of Li-S cell with UiO-66-S/Nafion hybrid-coated separator clearly showed the two cathodic peaks at 2.31 and 2.01 V, respectively. Meanwhile, these values were higher than those with pristine (2.24 and 1.89 V), UiO-66-S-coated (2.29 and 1.98 V), and Nafion-coated (2.28 and 1.97 V) separators. Furthermore, the CV curve of UiO-66-S/Nafion hybrid-coated separator cells revealed the sharper peaks and strongest intensities compared to other two cells. Thus, the UiO-66-S/Nafion hybrid-coated separator effectively prevented polysulfide shuttling, showing a rapid redox kinetics and good reversibility.[38]

In order to verify the capability of the UiO-66-S/Nafion hybrid coating layer in suppressing the polysulfide diffusion, simple visual identification was conducted in the permeation test as shown in the Fig. 5. Each separator was placed between

View Article Online
DOI: 10.1039/C8TA08845H

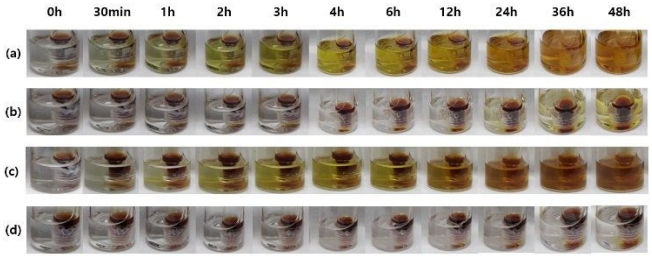

Fig. 5 Time-dependent visual identifications of long-chain polysulfide (Li_2S_6) diffusion in DOL/DME solution for (a) pristine, (b) Nafion-coated, (c) UiO-66-S-coated and (d) UiO-66-S/Nafion hybrid-coated separators.

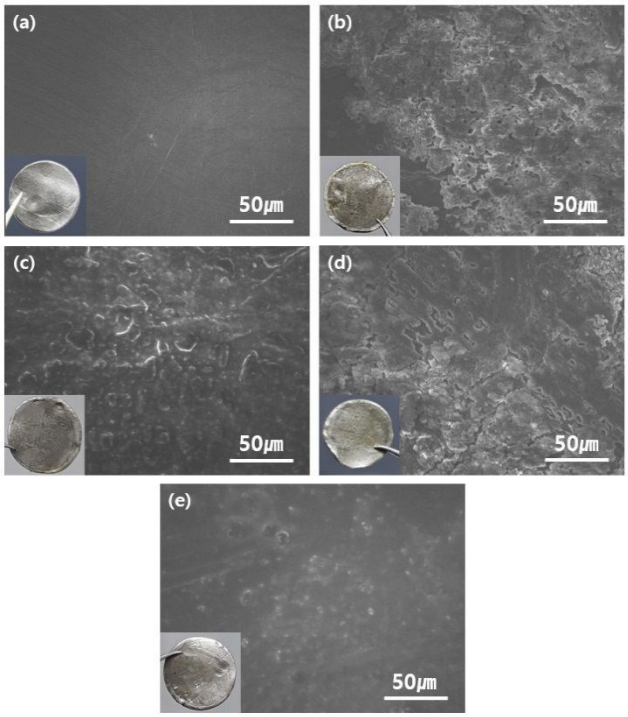

Fig. 6 Digital photographs (inset) and SEM images of Li metal surface (a) before and (b) after cycling process, and of (c) Nafion-coated and (d) UiO-66-S-coated and (e) UiO-66-S/Nafion hybrid-coated separators after cycling process.

the reddish polysulfide solution and empty electrolyte. Driven by concentration gradient, the polysulfides are spontaneously moved from the reddish solution to the empty electrolyte and the degree of diffusion is visually monitored by its color change. In the case of the pristine separator, polysulfide diffusion through the porous channel occurred immediately when it was immersed in the empty solution. The color was changed into yellowish within 30 minutes and turned into reddish in the whole bottle after 48 hours (Fig. 5a). By contrast, Nafion-coated separator showed a blocking effect on polysulfide diffusion due to the electrostatic repulsion. This separator maintained the original transparency of the empty solution for 12 hours (Fig. 5b). Then, it started to undergo a slight color change after 24 hours and finally, became completely yellow after 48 hours. The UiO-66-S-coated separator showed immediate color changes because of its open channels (Fig. 5c). The UiO-66-S/Nafion hybrid-coated separator remain transparent over 48 hours (Fig. 5d). The controlled pore size and sulfonic groups of UiO-66 enabled to successfully suppress the polysulfide diffusion.

In order to demonstrate the cycling performances enhanced by the suppressed polysulfide shuttling, we took digital photographs and SEM images of the Li metal surface before and after 40 charging/discharging cycles as shown in Fig. 6. The Li metal surface for the pristine separator became very rough, and there were a large amount of rounded particle (Figs. 6a and 6b), so called lithium dendrite, indicating that this Li-S cell suffered from severe polarization.[39] The Li metal surface for the UiO-66-S-coated separator also showed severe lithium dendrite formation (Fig. 6d). In comparison to the pristine separator and UiO-66-S-coated separator, the Nafion-coated and UiO-66-S/Nafion hybrid-coated separators showed the smooth surfaces of Li metal (Figs. 6c and 6e). In particular, the Li metal surface for the UiO-66-S/Nafion hybrid-coated separator remained almost intact after cycling test. For the part of separator, the fibers of the pristine separator became thick and some rounded particles were covered after cycling test (Figs. 1a and 1b). On the other hand, neither significant destruction in the morphology of MOF nor dramatic thickness variation was observed on the surface of the modified separator as shown in SEM images before and after cycling test (Figs. 1e and 1f and Fig. S8). The crystalline structure of UiO-66-S was also preserved despite the broadening of XRD peaks, which was due to the trapping of polysulfide inside the micropores of crystalline framework, for the UiO-66-S/Nafion hybrid-coated separator (Fig. 2a). As show in the digital photo images of each separator (Fig. S9), the modified separators showed lighter white colors and cleaner surfaces than those of pristine separator and, particularly, UiO-66-S/Nafion hybrid-coated separators exhibited almost negligible color change after cycling test. Consequently, sulfonic groups inside the UiO-66-S and Nafion acts as trapping the polysulfides within the cathode region by electrostatic force and reactivating the intercepted sulfur.[37, 42] XPS analysis was further conducted to characterize the interaction between polysulfides and modified separators (Fig S10). As shown in the S 2p peaks of UiO-66-S/Nafion hybrid-coated separator before and after immersing in long chain polysulfide solution, both spectra exhibited intensive peak at 169.2 eV which can be attributed to SO_3^- groups of Nafion and UiO-66-S.[49] After immersing in long chain polysulfides, the new peaks of S 2p at 168.2 and 166.7 eV were observed due to the formation of Li_2SO_4 and Li_2SO_3, respectively, confirming the strong interaction bewteen lithium ions of polysufide and SO_3^- groups of UiO-66-S/Nafion hybrid-coated separator. Moreover, S 2p peaks at below 164 eV were related to Li-S bond of polysulfides.[50] It notes that the dissolved long-chain polysulfides crossover the separator and are reduced into Li_2S and deposited on the lithium metal surface, which results in showing the unstable SEI layer and surface roughness. The Li-S cell undergoes severe polarization and lithium dendrite formation

due to the polysulfide deposition on the Li metal surface.[33, 40, 41] Thus, cycling performances and efficiencies can be improved effectively blocking the polysulfide shuttling and reactivating inactive sulfur by means of UiO-66-S/Nafion hybrid coatings.

Conclusion

In summary, UiO-66-S/Nafion hybrid-coated separator was fabricated to improve the performances of Li-S batteries. The functional group of sulfonic acid within UiO-66-S/Nafion hybrids played the roles of inhibiting polysulfide diffusion and dissolution by molecular sieving and electrostatic repulsion effect and of facilitating the redox kinetics of polysulfide conversion by the reduced charge transfer resistance. The Li-S cell with the UiO-66-S/Nafion hybrid-coated separator achieved discharge capacity of 1127.4 mAh g^{-1} at 0.1C and capacity retention of 75.5% over 200 cycles, which were much greater than those with pristine, Nafion-coated and UiO-66-S-coated separators. Among three Li-S cells, the one with UiO-66-S/Nafion modified separator exhibited the highest OCV retention of 98.4%, the lowest voltage hysteresis of 0.20eV, and the sharpest redox peaks, indicating its capability to improve the redox kinetics and reversibility. The prevention of polysulfide diffusion by the UiO-66-S/Nafion hybrids coated separator was confirmed analyzing time-dependent visual identification and the changes in the surface and morphology of Li anode and rGO/sulphur cathode after cycling test. Therefore, a functional separator coated by MOF/Nafion hybrids provide an effective strategy to inhibit the polysulfide shuttling effects and to improve the performances of Li-S cells.

Conflicts of interest

There are no conflicts to declare.

Acknowledgements

This research was supported by both a grant from R&D Program of the Korea Railroad Research Institute, Republic of Korea and Creative Materials Discovery Program through the National Research Foundation of Korea (NRF) funded by Ministry of Science and ICT(2018M3D1A1058744).

Notes and references

1. A. Manthiram, Y. Fu, S.-H. Chung, C. Zu and Y.-S. Su, *Chemical reviews*, 2014, **114**, 11751-11787.
2. Y. Diao, K. Xie, S. Xiong and X. Hong, *Journal of the electrochemical society*, 2012, **159**, A421-A425.
3. Y. Cui and Y. Fu, *Journal of Power Sources*, 2015, **286**, 557-560.
4. M. R. Busche, P. Adelhelm, H. Sommer, H. Schneider, K. Leitner and J. Janek, *Journal of Power Sources*, 2014, **259**, 289-299.
5. B. Zhang, X. Qin, G. Li and X. Gao, *Energy & Environmental Science*, 2010, **3**, 1531-1537.
6. L. Ji, M. Rao, S. Aloni, L. Wang, E. J. Cairns and Y. Zhang, *Energy & Environmental Science*, 2011, **4**, 5053-5059.
7. Q. Pang, D. Kundu, M. Cuisinier and L. Nazar, *Nature Communications*, 2014, **5**, 4759.
8. X. Liu, J. Q. Huang, Q. Zhang and L. Mai, *Advanced materials*, 2017, **29**, 1601759.
9. J. Wang, J. Yang, J. Xie and N. Xu, *Advanced materials*, 2002, **14**, 963-965.
10. Y. Yang, G. Yu, J. J. Cha, H. Wu, M. Vosgueritchian, Y. Yao, Z. Bao and Y. Cui, *ACS nano*, 2011, **5**, 9187-9193.
11. J. Zheng, J. Tian, D. Wu, M. Gu, W. Xu, C. Wang, F. Gao, M. H. Engelhard, J.-G. Zhang and J. Liu, *Nano letters*, 2014, **14**, 2345-2352.
12. R. Demir-Cakan, M. Morcrette, F. Nouar, C. Davoisne, T. Devic, D. Gonbeau, R. Dominko, C. Serre, G. Férey and J.-M. Tarascon, *Journal of the American Chemical Society*, 2011, **133**, 16154-16160.
13. S. H. Chung and A. Manthiram, *Advanced Functional Materials*, 2014, **24**, 5299-5306.
14. L. Shi, F. Zeng, X. Cheng, K. H. Lam, W. Wang, A. Wang, Z. Jin, F. Wu and Y. Yang, *Chemical Engineering Journal*, 2018, **334**, 305-312.
15. J.-Q. Huang, Q. Zhang, H.-J. Peng, X.-Y. Liu, W.-Z. Qian and F. Wei, *Energy & environmental science*, 2014, **7**, 347-353.
16. T. Z. Zhuang, J. Q. Huang, H. J. Peng, L. Y. He, X. B. Cheng, C. M. Chen and Q. Zhang, *Small*, 2016, **12**, 381-389.
17. I. Bauer, S. Thieme, J. Brückner, H. Althues and S. Kaskel, *Journal of Power Sources*, 2014, **251**, 417-422.
18. J. H. Cavka, S. Jakobsen, U. Olsbye, N. Guillou, C. Lamberti, S. Bordiga and K. P. Lillerud, *Journal of the American Chemical Society*, 2008, **130**, 13850-13851.
19. S. Biswas, J. Zhang, Z. Li, Y.-Y. Liu, M. Grzywa, L. Sun, D. Volkmer and P. Van Der Voort, *Dalton Transactions*, 2013, **42**, 4730-4737.
20. Q. Yang, A. D. Wiersum, P. L. Llewellyn, V. Guillerm, C. Serre and G. Maurin, *Chemical Communications*, 2011, **47**, 9603-9605.
21. M. Vijayakumar, N. Govind, E. Walter, S. D. Burton, A. Shukla, A. Devaraj, J. Xiao, J. Liu, C. Wang and A. Karim, *Physical Chemistry Chemical Physics*, 2014, **16**, 10923-10932.
22. K. M. Choi, K. Na, G. A. Somorjai and O. M. Yaghi, *Journal of the American Chemical Society*, 2015, **137**, 7810-7816.
23. Y. Geng, S. J. Wang and J.-K. Kim, *Journal of colloid and interface science*, 2009, **336**, 592-598.
24. S. A. Abbas, M. A. Ibrahem, L.-H. Hu, C.-N. Lin, J. Fang, K. M. Boopathi, P.-C. Wang, L.-J. Li and C.-W. Chu, *Journal of Materials Chemistry A*, 2016, **4**, 9661-9669.
25. R. Ghorbani-Vaghei, D. Azarifar, S. Daliran and A. R. Oveisi, *RSC Advances*, 2016, **6**, 29182-29189.
26. Y. M. Chung, Y. R. Lee and W. S. Ahn, *Bulletin of the Korean Chemical Society*, 2015, **36**, 1378-1383.
27. A. Gruger, A. Régis, T. Schmatko and P. Colomban, *Vibrational Spectroscopy*, 2001, **26**, 215-225.
28. M. L. Foo, S. Horike, T. Fukushima, Y. Hijikata, Y. Kubota, M. Takata and S. Kitagawa, *Dalton transactions*, 2012, **41**, 13791-13794.
29. Z. Lin, X. Cai, Y. Fu, W. Zhu and F. Zhang, *RSC Advances*, 2017, **7**, 44082-44088.
30. M.-K. Song, E. J. Cairns and Y. Zhang, *Nanoscale*, 2013, **5**, 2186-2204.

View Article Online
DOI: 10.1039/C8TA08843H

31. Y. X. Yin, S. Xin, Y. G. Guo and L. J. Wan, *Angewandte Chemie International Edition*, 2013, **52**, 13186-13200.
32. G. Zhou, in *Design, Fabrication and Electrochemical Performance of Nanostructured Carbon Based Materials for High-Energy Lithium–Sulfur Batteries*, Springer, 2017, pp. 75-94.
33. J.-Q. Huang, T.-Z. Zhuang, Q. Zhang, H.-J. Peng, C.-M. Chen and F. Wei, *Acs Nano*, 2015, **9**, 3002-3011.
34. V. Knap, D.-I. Stroe, M. Swierczynski, R. Teodorescu and E. Schaltz, *Journal of The Electrochemical Society*, 2016, **163**, A911-A916.
35. Z. Yuan, H.-J. Peng, T.-Z. Hou, J.-Q. Huang, C.-M. Chen, D.-W. Wang, X.-B. Cheng, F. Wei and Q. Zhang, *Nano letters*, 2016, **16**, 519-527.
36. D. Bresser, S. Passerini and B. Scrosati, *Chemical Communications*, 2013, **49**, 10545-10562.
37. H. J. Peng, D. W. Wang, J. Q. Huang, X. B. Cheng, Z. Yuan, F. Wei and Q. Zhang, *Advanced Science*, 2016, **3**, 1500268.
38. Y. Zhao, M. Liu, W. Lv, Y.-B. He, C. Wang, Q. Yun, B. Li, F. Kang and Q.-H. Yang, *Nano Energy*, 2016, **30**, 1-8.
39. A. Pei, G. Zheng, F. Shi, Y. Li and Y. Cui, *Nano letters*, 2017, **17**, 1132-1139.
40. L. Zhang, M. Ling, J. Feng, L. Mai, G. Liu and J. Guo, *Energy Storage Materials*, 2018, **11**, 24-29.
41. J. Zheng, M. Gu, H. Chen, P. Meduri, M. H. Engelhard, J.-G. Zhang, J. Liu and J. Xiao, *Journal of Materials Chemistry A*, 2013, **1**, 8464-8470.
42. Y. Jiang, F. Chen, Y. Gao, Y. Wang, S. Wang, Q. Gao, Z. Jiao, B. Zhao and Z. Chen, *Journal of Power Sources*, 2017, **342**, 929-938.
43. S. Bai, X. Liu, K. Zhu, S. Wu and H. Zhou, *Nature Energy*, 2016, **1**, 16094.
44. M. Li, Y. Wan, J.-K. Huang, A. H. Assen, C.-E. Hsiung, H. Jiang, Y. Han, M. Eddaoudi, Z. Lai and J. Ming, *ACS Energy Letters*, 2017, **2**, 2362-2367.
45. S. Suriyakumar, M. Kanagaraj, M. Kathiresan, N. Angulakshmi, S. Thomas and A. M. Stephan, *Electrochimica Acta*, 2018, **265**, 151-159.
46. F. Wu, S. Zhao, L. Chen, Y. Lu, Y. Su, Y. Jia, L. Bao, J. Wang, S. Chen and R. Chen, *Energy Storage Materials*, 2018, **14**, 384-391.
47. Y. Guo, M. Sun, H. Liang, W. Ying, X. Zeng, Y. Ying, S. Zhou, C. Liang, Z. Lin and X. Peng, *ACS Applied Materials & interfaces*, 2018, **10**, 30451-30459.
48. D. H. Lee, J. H. Ahn, M. S. Park, A. Eftekhari, D. W. Kim, *Electrochimica Acta*, 2018, **283**, 1291-1299.
49. F. Zeng, Z. Jin, K. Yuan, S. Liu, X. Cheng, A. Wang, W. Wang and Y.-s. Yang, *Journal of Materials Chemistry A*, 2016, 4, 12319-12327
50. Y. Jung and B. Kang, *Physical Chemistry Chemical Physics*, 2016, 18, 21500-21507.